



## Optimization of Ciprofloxacin Sorption on Chitosan-Carbon Nanotube Composite Using Response Surface Methodology: Process Variables and Affinity Evaluation

Siphesihle M. Khumalo<sup>1\*</sup>, Babatunde F. Bakare<sup>2</sup>, Sudesh Rathilal<sup>1</sup>

<sup>1</sup> Green Engineering Research Group, Department of Chemical Engineering, Durban University of Technology, Durban 4001, South Africa

<sup>2</sup> Environmental Pollution and Remediation Research Group, Department of Chemical Engineering, Mangosuthu University of Technology, Durban 4031, South Africa

Corresponding Author Email: [21752152@dut4life.ac.za](mailto:21752152@dut4life.ac.za)

Copyright: ©2023 IIETA. This article is published by IIETA and is licensed under the CC BY 4.0 license (<http://creativecommons.org/licenses/by/4.0/>).

<https://doi.org/10.18280/ijdne.180610>

### ABSTRACT

**Received:** 18 July 2023

**Revised:** 22 September 2023

**Accepted:** 31 October 2023

**Available online:** 26 December 2023

#### Keywords:

*ciprofloxacin, central composite design, pH, chitosan, carbon nanotubes, response surface methodology, sorption, optimization, wastewater treatment*

The need to mitigate the toxicological impact of antibiotics in wastewater necessitates advancements in treatment technologies. This study endeavors to refine the sorptive removal of ciprofloxacin (CIP) using chitosan-carbon nanotube (chitosan-CNT) composite, leveraging response surface methodology (RSM) for process optimization. The motivation is anchored in addressing the insufficiencies of conventional wastewater treatments to fully eliminate antibiotics, with repercussions for human health and biota. Employing the central composite design (CCD) within RSM, the study rigorously ascertains optimal combinations of process variables including contact time, adsorbent dosage, initial CIP concentration, and pH levels, through comprehensive statistical analysis. It was observed that the solution pH critically governs the adsorption efficiency, influencing the surface charge of the adsorbent and the speciation of CIP. The optimized conditions were determined as a pH of 6.3, an adsorbent dose of 1.06 g/L, contact time of 352 min, and an initial CIP concentration of 39 mg/L, under which a CIP removal efficiency of 64.3% was achieved, with a standard deviation of 0.396%. The model's robustness was corroborated by a high coefficient of determination ( $R^2 = 0.997$ ), satisfactory adjusted  $R^2$  (0.9950) and predictive  $R^2$  (0.9952) values. The study's outcomes advocate for the adjustment of pH as a critical consideration in the sorptive process and underscore the potential of chitosan-CNT composites as a sustainable, green technology for antibiotic remediation in wastewater treatment. The findings mark a stride towards refining adsorption-based wastewater treatment protocols, thus contributing to the broader objective of environmental conservation and public health protection.

## 1. INTRODUCTION

Pharmaceutical compounds (PCs) have garnered increasing scrutiny due to their pervasive presence in various aqueous environments, including surface water [1-3], groundwater [2], and treated water supplies [2, 4, 5]. These contaminants, now recognized as emerging environmental concerns, are highlighted by the persistent and mobile fluoroquinolone class of antibiotics, which exhibit resistance to biodegradation at both low and significant concentrations [6]. Within this class, ciprofloxacin (CIP), a broad-spectrum antibiotic, stands out due to its extensive application in treating bacterial infections across human, animal, and plant health sectors [7, 8]. Its ubiquity in the environment and subsequent detection in water bodies [2, 4-6] has raised alarms due to its ability to foster antibiotic resistance through suboptimal degradation during water treatment processes. Furthermore, exposure to CIP-contaminated water has been associated with adverse human health outcomes, including headaches, skin diseases, and gastrointestinal disturbances [8]. The bioaccumulation of CIP also impinges on plant growth rates by adversely impacting

photosynthesis [9, 10].

The current wastewater treatment technologies within South African contexts have been shown to be insufficient for the complete removal of CIP from water, indicating a pressing need for enhanced remediation methods [4, 5]. Among the various strategies pursued, solid-liquid phase adsorption, particularly leveraging chitosan-based composites, has been identified as a promising approach [6, 11-16]. Hitherto, studies are being conducted on the application of different adsorbents such as shell-core chitosan adsorbent [17], activated carbon from *Prosopis juliflora* [18], chitosan modified rubber [19], zeolites [20] etc on the removal of antibiotics from aqueous environments. Despite extensive investigations into the kinetics, isotherms, and thermodynamics of antibiotic adsorption, studies optimizing the adsorption process parameters remain relatively sparse. This study seeks to fill this gap by focusing on the parametric optimization of CIP removal using chitosan-CNT composite microbeads as a sustainable adsorbent.

Chitosan, the second most abundant biopolymer after cellulose, is produced through the deacetylation of chitin in a

basic medium, primarily sourced from crustaceans and other organisms like insects and fungi [8, 21]. Its inherent positive charge, arising from hydroxyl (-OH) and amino (-NH<sub>2</sub>) groups as depicted in Figure 1 [15, 22], provides excellent chelating sites for the targeted removal of pollutants from water. These functional groups also render chitosan amenable to various chemical modifications, enhancing its potential as an adsorbent for PC remediation [15, 22, 23]. Chitosan-based adsorbents are favored for their low processing costs, hydrophilicity, biodegradability, non-toxicity, and high affinity for a range of biomacromolecules [8, 15, 24]. However, the application of unmodified chitosan is limited due to its solubility in acidic environments, poor mechanical strength, and challenges in controlling pore size [25]. These limitations can be addressed by incorporating carbon nanotubes (CNTs), which provide heightened tensile strength and stability to the composite [26, 27]. Acid-functionalized CNTs promote the formation of a strong bond with chitosan through hydrogen bonding, which facilitates an improved interfacial strength of the composite. The role of CNTs in the sorption of antibiotics, attributed to  $\pi$ - $\pi$  interaction mechanisms, further underscores their suitability as nanofillers in the synthesis of chitosan composites for water treatment applications [28, 29].

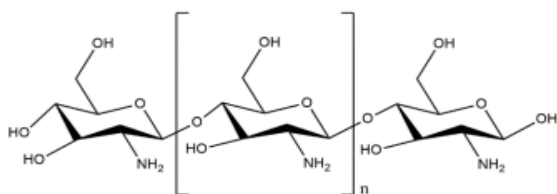


**Figure 1.** Schematic presentation of chitosan structure

In light of the literature focusing predominantly on adsorption kinetics and isotherms [11, 13, 14], the paramount objective of this study is to rigorously analyze the efficacy of chitosan-CNT beads for CIP removal under optimized conditions. The optimization parameters considered encompass contact time, initial CIP concentration, pH, and adsorbent dosage. The central composite design (CCD) within the framework of response surface methodology (RSM) is employed to determine the optimum operating conditions and to establish a predictive model for CIP adsorption onto chitosan-CNT composites.

## 2. MATERIALS AND METHODS

### 2.1 Materials

For this study, all chemicals used were of analytical grade, no further purification was done. Chitosan powder from shrimp shells with a degree of deacetylation of  $\geq 75\%$ , sodium hydroxide pellets (NaOH), methanol (CH<sub>3</sub>OH), sulphuric acid (H<sub>2</sub>SO<sub>4</sub>) was supplied by Sigma-Aldrich, South Africa. Glacial acetic acid was supplied by Shalom laboratories, Durban, South Africa, multi-wall carbon nanotubes and CIP antibiotic (C<sub>17</sub>H<sub>18</sub>FN<sub>3</sub>O<sub>3</sub>) were supplied by Lasec laboratories, Durban, South Africa.

### 2.2 Carbon nanotubes (CNTs) functionalisation

The natural chemistry of pristine CNTs is that they bundle together and become inseparable in solutions. Yet the success

of CNT application in any technology within the wastewater treatment sphere is strongly dependent on the capability of disbanding them into individual nanotubes, thus making them homogenous and stable suspensions [30]. Hence, CNT surface modification engineering is crucial for advanced CNT surface properties. For the current work, CNT modification was done by soaking a specific amount of CNTs in a solution of concentrated sulfuric acid (99%) and nitric acid (65%) at a volume ratio of 1:2, respectively for 24 hours. The liquid-phase oxidation of CNTs using an acid containing oxygen molecules, results in the attachment of functional groups such as carboxylic and hydroxyl groups on the CNT surface which are essential for contaminant removal in the aqueous environment [30]. Thereafter, the acid functionalized CNTs were rinsed with deionized water until a pH of 7 was achieved for the filtrate. The pH of the filtrate was measured using a HANNA HI 9828 pH meter. Moreover, CNTs were functionalized to obtain a more hydrophilic surface as compared to pristine CNTs.

### 2.3 Chitosan-CNT adsorbent preparation

The chitosan-CNT composite was prepared by dissolving 100g of chitosan in 400mL of 1% v/v of glacial acetic acid solution, it is worth noting that chitosan does not dissolve in water but in weak acidic aqueous environments. Thereafter, the chitosan-glacial acetic acid mixture was vortexed using a magnetic stirrer at 200 rpm for 24 hours at room temperature to allow for complete dissolution of chitosan due to its low solubility thus prolonged periods of agitation are necessary. During vortexing, the mixture of chitosan-glacial acetic acid was covered with aluminium foil to minimise any evaporation since glacial acetic acid is relatively volatile. Thereafter, 5wt.% (with respect to chitosan) of functionalised multiwall CNTs were added into the chitosan-glacial acetic acid mixture, which was followed by vortexing the acid mixture at 200 rpm for 2 hours. This was done to obtain a homogeneous distribution of CNTs in the mixture. The viscous chitosan-CNT mixture was allowed to degas in a vacuum desiccator at room temperature until all air bubbles disappeared (i.e., disappearance of air pockets within the viscous mixture). Chitosan-CNT microbead composite was synthesised by adding the viscous chitosan-CNT gel dropwise in a solution of 15wt.% NaOH and 95% (v/v) methanol at a volume ratio of 4:1, respectively, using a 10-mL syringe which precipitated into chitosan-CNT beads. The chitosan-CNT beads were soaked in the NaOH-methanol solution for 24hours, then rinsed with deionised water until a pH of 7 was obtained prior to being dried at 55°C for 12hours.

### 2.4 Ciprofloxacin (CIP) batch adsorption studies

The sorption of CIP on chitosan-CNT was evaluated by batch experiments with initial input variables in the range of, contact time (30-480min), chitosan-CNT dosage (0.05-1.5g/L), initial CIP concentration (10-50mg/L), and pH (2-10). It is worth noting that screening experiments were conducted to determine experimental variables as well as interactions that have significant influence on the responses. Factors in CCD within the framework of RSM were examined at two levels, i.e., -1, +1. The range between the levels denotes the broadest interval in which the factors were varied for the current study based on the screening experiments which were conducted prior. Moreover, on the basis that urban wastewater pH varies

over a wide range depending on the point source, it was necessary to investigate the efficiency of chitosan-CNT adsorbent on the sorption of CIP over a wide range of pH. Adsorption studies were conducted using a sample volume of 100mL for each corresponding initial condition as designed in RSM (see Table 1 in the supplementary data). Samples agitation was done using a Stuart orbital shaker SSL1 from Lasec laboratories, Durban, South Africa; the solution pH was measured using a HANNA HI 9828 pH meter, adsorbent and adsorbate weights were measured using a Labotec J series analytical balance. At the end of each experimental run, samples were filtered using a 0.45µm syringe filter and transferred into a 10mL sample tube. The filtered samples were then centrifuged at 5000rpm for 10minutes, thereafter, a supernatant solution of the centrifuged sample was analysed for the residual CIP concentration using a UV-vis spectrophotometer (UV-1900i, Shimadzu, South Africa) at a wavelength of 272nm. The amount of CIP adsorbed by the model adsorbent was determined using Eq. (1).

$$\eta = \frac{C_0 - C_t}{C_0} \times 100\% \quad (1)$$

where,  $\eta$  is the percentage removal of ciprofloxacin from solution,  $C_0$  and  $C_t$  are the initial and final (i.e., at time  $t$ ) concentrations of CIP in mg/L.

## 2.5 Experimental design and model evaluation

To ascertain the optimum conditions for CIP sorption in chitosan-CNT composite as a model adsorbent from aqueous solutions, the CCD within the RSM framework in Design Expert version 11 was used to obtain the number of experimental runs (Table 1). For the current study, process optimization was achieved by determining the interaction between four independent process variables i.e., contact time (A), chitosan-CNT dose (B), initial CIP concentration (C), and pH (D) towards CIP removal as a single output response. The application of the CCD within the framework of RSM allows for a large number of experiments to be conducted in parallel and it is more efficient for up to five factors [31]. Moreover, the CCD allows for sensitive data for testing the lack of fit without involving a large number of design points which has cemented its application in process optimization studies [32, 33]. The codes, ranges, and levels of the investigated parameters which were considered for the CIP removal model optimization are as depicted in Table 1.

**Table 1.** Codes, ranges, and levels of independent variables of composite design in RSM

Range and Level of Factors			
Factor	Code	Low -1	High +1
Contact time (min)	A	30	480
Chitosan-CNT dose (g/L)	B	0.05	1.5
Initial CIP conc. (mg/L)	C	10	50
pH	D	2	10

The optimized conditions of the response output in terms of CIP removal (Y) with respect to the independent variables was approximated using the following empirical second-order polynomial model within the framework of RSM (2).

$$Y = \beta_0 + \sum_{i=1}^k \beta_i X_i + \sum_{i=1}^k \beta_{ii} X_i^2 + \sum_{i=1}^{k-1} \sum_{j=i+1}^k \beta_{ij} X_i X_j + \varepsilon \quad (2)$$

$$X_i = \left( \frac{z_i - z_0}{\Delta z_i} \right) \beta_d \quad (3)$$

where,  $Y$  is the predicted response,  $X_i$  and  $X_j$  are the input variables,  $\beta_0$ ,  $\beta_i$ ,  $\beta_{ii}$ , and  $\beta_{ij}$ , are the regression constants for intercept, linear coefficient, quadratic coefficient, and coefficient of regression, respectively;  $k$  denotes the number of factors studied and optimized by the experiment and  $\varepsilon$  accounts for the random error [32];  $z_i$  and  $z_0$  denotes the code and uncoded values of the  $i$  th independent variable, respectively;  $\beta_d$  is the major coded limit value in the matrix for each variable, and  $\Delta z_i$  is the step-change codification of the value between the low level (-1) and high level (+1). Codification of independent variables was conducted solely for the purpose of normalising the variables. Independent variables may have unique units and orders of magnitude. The codification ensures that all independent variables affect the specified responses evenly.

The quality of the fitted model was evaluated by applying the analysis of variance (ANOVA) which compares the variation due to the change in the combination of variable levels with the variation due to random errors inherent to the measurements of the generated responses [34]. Hence, from such comparison it was possible to evaluate the significance of the regression to predict the output response considering the sources of experimental variance.

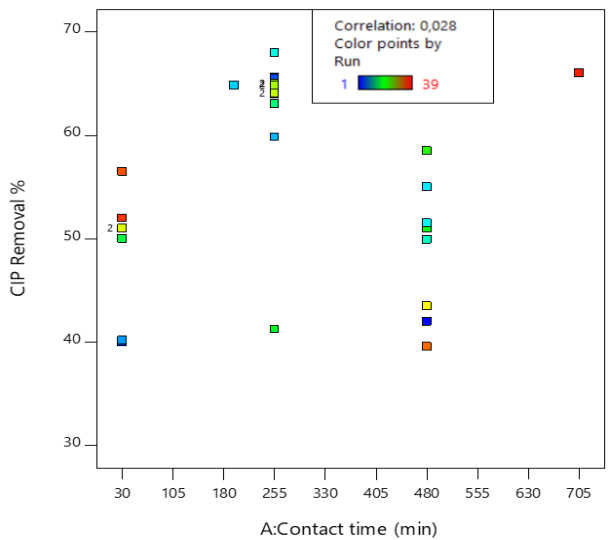
## 3. RESULTS AND DISCUSSION

### 3.1 Influence of input variables on the removal of CIP in RSM

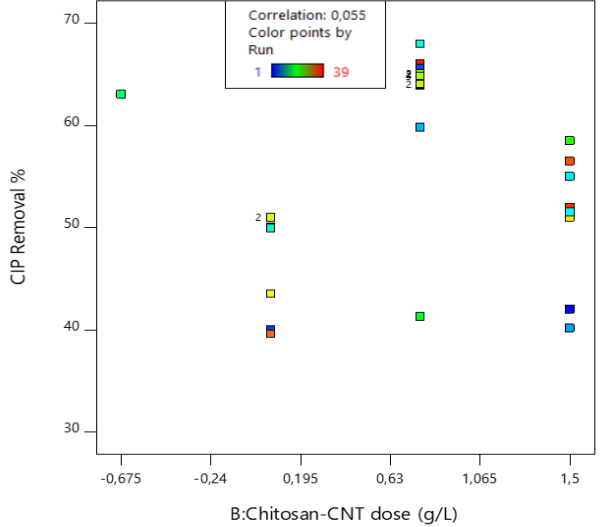
In RSM, the effect of process variables on the output response can be measured using a scatterplot within the framework of RSM as a statistical analysis tool. In ascertaining the effect of each process variable (contact time, chitosan-CNT dose, CIP initial concentration, and pH) on the response variable (CIP removal), scatterplots of the response versus each process variable were plotted as depicted in Figure 2. It is worth noting that a linear relationship between the process variable and the response was first assumed allowing the gradient of the plots to represent the correlation between each process variable and the response. According to Madondo et al. [33] a positive correlation is an indication that there is direct proportionality between the process variable and the corresponding response output. On the other hand, a negative correlation indicates that indirect proportionality exists between the process variables and the response output. The findings of the current study recorded unique correlations for each process variable i.e., 0.028 (contact time), 0.055 (chitosan-CNT dose), -0.254 (initial CIP concentration), and 0.304 (pH). Hence, the RSM results suggest that, increasing the contact time, adsorbent dose (chitosan-CNT), and pH result in an increase in CIP removal. However, an increase on the initial CIP concentration results in a decrease in CIP removal by adsorption using chitosan-CNT as a model adsorbent. Based on the absolute values of the obtained correlations, it is evident that pH was the most influential factor in the removal of CIP by chitosan-CNT followed by the adsorbent dose and contact time while the initial CIP concentration demonstrated the least effect.

It is noted that the scatterplot model analysis is solely based on the assumption that there is a linear relationship between

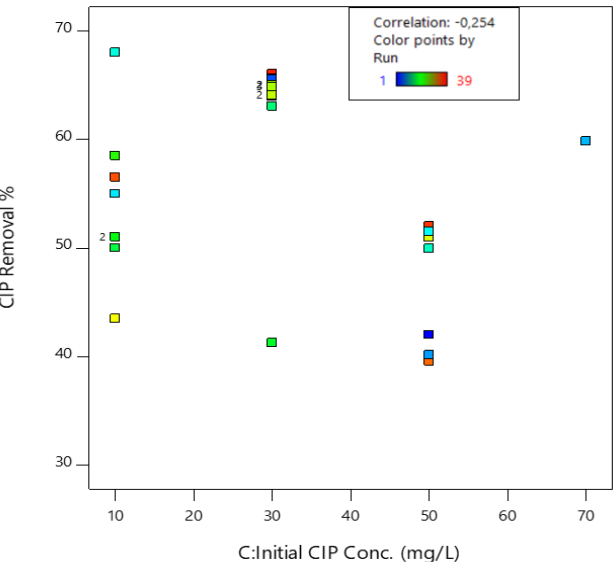
factors investigated and the response output which serves as a starting point for statistical analysis [33]. Hence, the validity of the linear relationship between the input factors and the response output had to be validated by performing the analysis of variance between the dependent variable i.e., Y and independent variables i.e., A, B, C, and D.



(a)



(b)



(c)

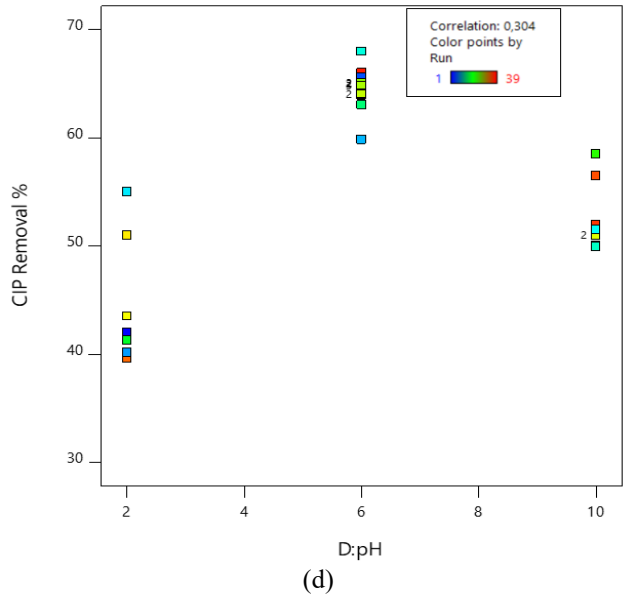


**Figure 2.** (a) Effect of contact time on CIP removal; (b) Effect of chitosan-CNT dose on CIP removal; (c) Effect of initial CIP concentration on CIP removal; (d) Effect of pH on CIP removal

### 3.2 Analysis of variance (ANOVA)

The ANOVA was performed to ascertain the significance of the reduced cubic model (4) as well as the interactions between the dependent variable, Y and the four independent variables A, B, C, and D. The CIP removal polynomial predictive model was evaluated by considering four imperative statistical parameters i.e., the sum of squares, mean square, F-value, and p-value as depicted in Table 2 at 95% confidence level to appraise its statistical significance. Generally, the significance of any process related parameter can be analysed by applying the sum of squares value. Higher sum of square values implies a significant effect of the corresponding variable in the context of a typical process. From the ANOVA findings, pH recorded the highest sum of squares value of 244.44, which implies that pH had a significant effect on CIP removal when compared to contact time (1.87), adsorbent dose (83.00), and initial CIP concentration (123.73).

It is imperative to note that the ANOVA results are congruent with the scatterplot analysis which implied that pH was the most influential factor in CIP removal.

$$Y = 64.64 - 2.60A + 2.47B - 2.60C + 4.21D + 0.142AB - 0.5217AD - 1.82BC - 0.3905BD + 1.16CD + 1.67A^2 + 0.86B^2 - 18.82D^2 + 3.11AB^2 \quad (4)$$

For the reduced cubic CIP predictive model, the significance of a parameter was evaluated by its F-value which should be higher than the rest and its p-value (i.e., probability value) should be less than 0.05 [35]. From the ANOVA results, components for the CIP removal predictive model had F-values in the order of 596.05 (pH) > 301.72 (initial CIP concentration) > 202.40 (adsorbent) > 4.57 (contact time) and p-values of p < 0.0001 for pH, adsorbent dose, and initial CIP concentration as well as a p-value of 0.0430 for contact time. As such, the ANOVA statistical results suggest a higher degree of fit for the reduced cubic model for the CIP removal as the output response, and that selected combinations are highly significant at 95% confidence level. Furthermore, the

model p-value of <0.0001 and F-value of 543 implies that the CIP removal model is significant. Within the framework of ANOVA, p-values less than 0.05 indicate that model terms are significant i.e., A, B, C, D, AB, AC, AD, BC, BD, CD, A<sup>2</sup>, B<sup>2</sup>, D<sup>2</sup>, and AB<sup>2</sup>. Additionally, the lack of fit F-value of 2.08 implies the lack of fit is not significant relative to the pure error. Therefore, there is a 10.26% chance that a lack of fit with an F-value of 2.08 could occur due to noise thus cementing the goodness of fit of the reduced cubic model. In other words, the

lack of fit p-value of >0.05, implies the insignificance of the models' failure and the considerable effects of the independent parameters on CIP removal.

Furthermore, the goodness of fit of the reduced cubic model was tested by means of the fit statistics (Table 3) within the framework of ANOVA. The overall significance of the model was measured by considering both the coefficient of determination, R<sup>2</sup> as well as the adjusted coefficient of determination, adjusted R<sup>2</sup> [31].

**Table 2.** ANOVA results for CIP removal

Source	Sum of Squares	Degree of Freedom	Mean Square	F-Value	P-Value	Significance
Model	3118.71	14	222.77	543	<0.0001	significant
A-contact time	1.87	1	1.87	4.57	0.0430	
B-chitosan-CNT dose	83.00	1	83.00	202.40	<0.0001	
C-initial CIP conc.	123.73	1	123.73	301.72	<0.0001	
D-pH	244.44	1	244.44	596.05	<0.0001	
AB	2.29	1	2.29	5.58	0.0266	
AC	3.67	1	3.67	8.94	0.0063	
AD	1.43	1	1.43	3.48	0.0744	
BC	44.59	1	44.59	108.74	<0.0001	
BD	2.05	1	2.05	5.01	0.0348	
CD	18.00	1	18.00	43.89	<0.0001	
A2	3.14	1	3.14	7.66	0.0107	
B2	9.13	1	9.13	22.27	<0.0001	
D2	448.54	1	448.54	1093.74	<0.0001	
AB2	2.68	1	2.68	6.53	0.0174	
Residual	9.84	24	0.4101			
Lack of fit	4.54	7	0.6492	2.08	0.1026	insignificant
Pure error	5.30	17	0.3117			
Corrected total	3128.55	38				

**Table 3.** Model fit statistics for the CIP removal

Statistical Parameter	Value
Standard deviation	0.6404
Mean	57.89
Coefficient of variance (%)	1.11
Coefficient of determination (R <sup>2</sup> )	0.9969
Adjusted R <sup>2</sup>	0.9950
Predicted R <sup>2</sup>	0.9552
Adequate precision	70.4865

R<sup>2</sup> is a statistical parameter which measures the total variation of predicted values to the mean. For a model with a good prediction efficiency, the value of R<sup>2</sup> must be closer to 1 [31, 33]. Hence, the R<sup>2</sup> value of 0.9969 suggest that the reduced cubic model satisfactorily predicts the CIP removal efficiency. It is worth noting that values of R<sup>2</sup> increases with an increase in the number of terms in the model regardless of the significance of the term [31, 35]. Therefore, the model efficiency cannot be tested solely by R<sup>2</sup>. The adjusted R<sup>2</sup> is another significant statistical parameter in the context of the model goodness of fit test. According to Alimohammadi et al. [35], the adjusted R<sup>2</sup> corrects the R<sup>2</sup> value for a sample size and the number of terms in the model. In other words, if there are many terms in the model and the sample size is not large, the value of the adjusted R<sup>2</sup> will not increase with the number of terms but it will be smaller than the value of R<sup>2</sup>. For the current study, the values of both R<sup>2</sup> (0.9969) and adjusted R<sup>2</sup> (0.9950) are relatively high close to 1, suggesting that the reduced cubic model satisfactory predicts the desired response with minimal deviations of 0.6404 in terms of the standard deviation. Moreover, the adequate precision which measures the signal to noise ratio and for a good prediction model a ratio

that is greater than 4 is desirable [31]. The obtained adequate precision value of 70.487 (Table 3) is a clear indication of an adequate signal. Therefore, the model can be used to navigate the design space of the experimental study [31].

### 3.3 Model validation

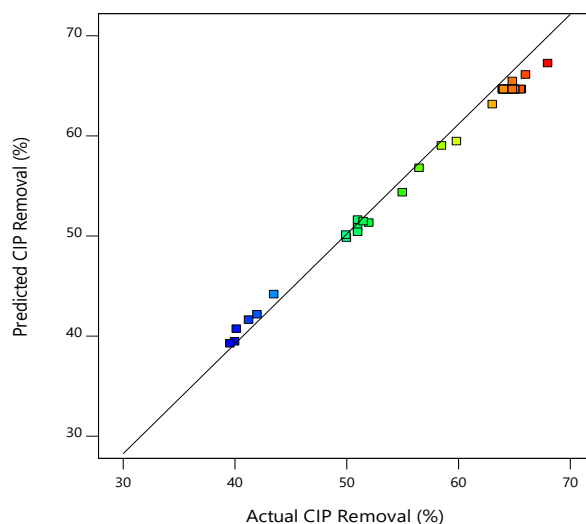


**Figure 3.** Predicted versus actual CIP removal efficiency

The reduced cubic model was validated by conducting the diagnostic test in terms of the plot of externally studentized results versus experimental runs as well as the plot of the predicted % CIP removal versus the actual % CIP removal. It

is worth noting that, the residual analysis is imperative for model development to confirm the ANOVA results. According to Montgomery [31] and Khumalo et al. [32] for a good prediction, a plot of the response values of the predicted versus actual should be randomly scattered not far from the 45° line (Figure 3). Groups of points above or below the 45° line indicate areas of over or under prediction. Therefore, for the current study it is apparent that in Figure 3, data points are randomly distributed closer to the 45° line implying a significant correlation between the independent variables and responses. As such, the model demonstrates insignificant errors within the bounds of the operating parameters.

Furthermore, the diagnostics plot in terms of the externally studentized residuals versus experimental runs (Figure 4) was applied to check for lurking variables that may have influenced the response during the experiment. A model with a good prediction efficiency is characterised with a random scatter plot as depicted in Figure 4. On the other hand, a trend indicates a time-related variable lurking in the background. Studentized residuals allow comparison of differences between the observed values and predicted target values in a typical regression model across different predictor values. In other words, an externally studentized residual, is the deleted residual divided by its estimated standard deviation and it is effective for detecting outlying observations. Therefore, if an observation has an externally studentized residual greater than 3, it is called an “outlier”. An “outlier” or an observation with a high leverage exerts influence on the fitted model, biasing the model outputs. As such, for the reduced CIP removal cubic model, no outliers were observed i.e., all externally studentized residuals were within the residual limits suggesting that the response do not require any transformation [31].

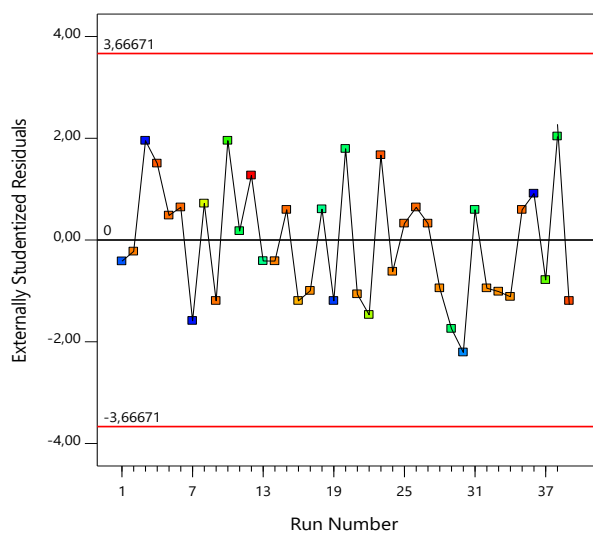


**Figure 4.** Externally studentized residuals versus run number

### 3.4 The interaction effect of pH on CIP removal

Generally, the solution pH is an imperative parameter to monitor and control in wastewater treatment processes particularly by solid-liquid adsorption due to its ability to change the surface charge of the adsorbent, and speciation distribution of ionizable organic contaminants [6, 14]. Therefore, for the current study, it was necessary to study the effect of interaction between pH and contact time (Figure 5), initial CIP concentration (Figure 6) as well as chitosan-CNT

dose (Figure 7) on CIP removal. CIP is characterised with a carboxylic acid functional group (-COOH) and an amine functional group (-NH<sub>2</sub>) on the piperazine moiety with corresponding pK<sub>a</sub> values of 6.1 and 8.7, respectively [6]. It is apparent from Figures 5-7 that the highest CIP removal was achieved at a solution pH of 6, and any pH variation above or below 6 hindered the adsorption of CIP on chitosan-CNT regardless of a change in contact time (Figure 5), adsorbent dose (Figure 6), and initial concentration (Figure 7). The observed behaviour in the affinity of chitosan-CNT adsorbent on CIP is attributed to the mere fact that at a pH of less than 6.1, CIP is positively charged, thus the interaction between CIP and the negatively charged chitosan-CNT surface becomes stronger favouring the affinity of chitosan-CNT towards CIP. Moreover, within the design space of the current experimental study at pH < 6, the removal of CIP decreased which can be attributed to the fact that, at low pH conditions, the hydrophilic functional groups (i.e., -OH, -NH<sub>2</sub>, and -COOH) on the chitosan-CNT adsorbent surface become positively charged due to protonation [14]. As such, lower solution pH conditions favour electrostatic repulsion between CIP and chitosan-CNT adsorbent, thus resulting in weaker bonding between the model adsorbent and adsorbate. Thus, an increase in pH resulted in a decrease in the positive charge of the adsorbent surface, subsequently promoting electrostatic interaction between the model contaminant and the adsorbent. The low removal efficiencies of CIP under acidic aqueous environments can also be ascribed to the increase in chitosan solubility with a decrease in solution pH [36].

Furthermore, the percentage removal of CIP decreased with an increase in pH above 6, i.e., pH of 10 despite any variation in terms of contact time, adsorbent dose, and initial CIP concentration. The observed behaviour can be attributed to the effect of solution pH on the speciation of the model contaminant, i.e., CIP. As reported by Wang et al. [6] and Verma et al. [14], CIP has a pK<sub>a</sub> value of 8.7 which implies that, at pH conditions greater than 8.7 the CIP surface can be negatively charged, hence the interaction between the negatively charged CIP and chitosan-CNT adsorbent surface becomes significantly weak thus compromising its affinity towards CIP. In other words, the increase in solution pH above 8.7 weakens the CIP cationic  $\pi$  bonding.

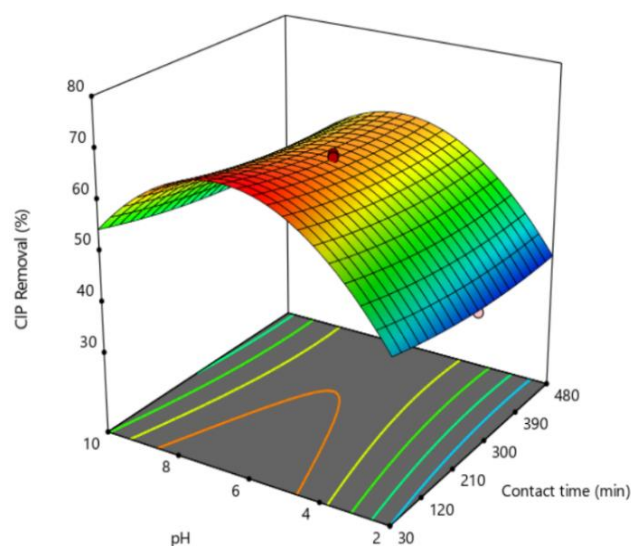


**Figure 5.** Effect of interaction between pH and contact time on CIP removal

From Figure 5, the highest CIP removal of 64.25% was achieved at a contact time of 255 minutes and pH 6. In a typical solid-liquid adsorption process, the rate of adsorption increases with an increase in contact time due to free adsorption sites on the surface of the model adsorbent. However, it was anticipated that, after a definite period, the adsorption rate decreases due to the unavailability of active sites on the adsorbent surface. Therefore, the findings of the study suggest that for the investigated system, all chitosan-CNT active sites were occupied by CIP at a contact time of 255 minutes, hence, no further adsorption of CIP was feasible after 255 minutes for a solution pH of 6.

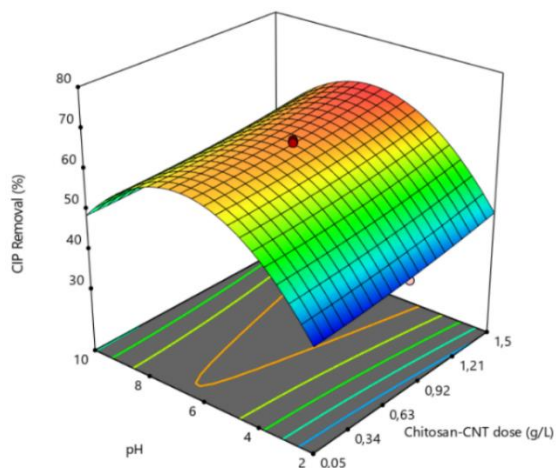


**Figure 6.** Effect of interaction between pH and chitosan-CNT dose on CIP removal

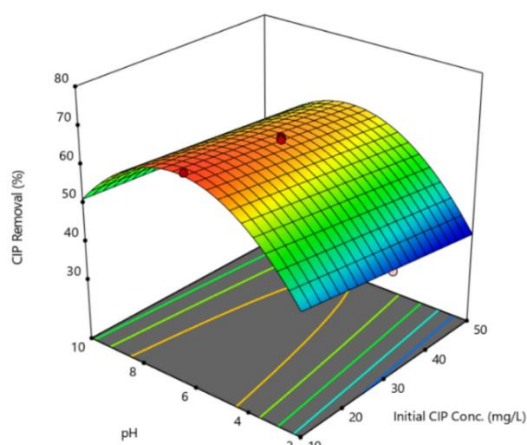


**Figure 7.** Effect of interaction between pH and initial CIP concentration on CIP removal

Furthermore, the adsorbent dose was investigated on the basis that an increase in the adsorbent dose provides large surface area and more active sites for the adsorption. From Figure 6, it is apparent that the highest CIP removal was achieved for a chitosan-CNT dose of 0.775g/L. The results obtained suggest that an increase in chitosan-CNT dose beyond 0.775g/L did not improve the adsorption capacity of CIP in the context of the investigated system. The plateau in Figure 6 in relation to chitosan-CNT dose variation is evident that beyond the adsorbent dose of 0.77g/L, the CIP removal was not affected any further. Moreover, the findings presented in Figure 7 suggest that an increase in the initial concentration of CIP beyond 30mg/L did not improve the adsorption of CIP

by chitosan-CNT adsorbent. As such, the observed trend can be ascribed to the decrease in active sites for adsorption on the surface of the adsorbent. Therefore, any further increase on the initial CIP concentration will compromise the adsorption efficiency due to lack of new active sites.

### 3.5 Numerical optimization

Numerical optimization was employed within the framework of RSM using Design Expert version 11, aimed at ascertaining the optimum operating conditions in terms of contact time (352min), adsorbent dose (1.06g/L), initial CIP concentration (38.8mg/L), and solution pH (6.3) for maximum CIP removal as depicted in Figure 8. The system gave 100 conditional solutions with 100% desirability at 95% confidence level. For the current study, the desirability function within the framework of RSM was applied on the basis that the quality of the responses of the adsorption process having four input variables is completely unacceptable if one of the variables is outside of the desirable limit. As such, by employing the desirability function it allows to find operating conditions that ensure compliance with the criteria of all the involved responses at the same time proving the best value of compromise in the desirable joint response as eluded by Candiotti et al. [37]. For the sorption of CIP on chitosan-CNT composite this was achieved by converting the multiple responses into a single one, combining the individual responses into a composite function followed by its optimization within the framework of RSM [37]. In RSM, an individual desirability function for each response was created using the fitted response models thus establishing the optimization criteria. It is worth noting that, the desirability function opts for the values between 0 (undesirable response) and 1 (completely desirable response). Desirability intermediate values may indicate more or less desirable responses. As the 100% desirability reported for the present study, suggest that the conditions present in the ramp plot in Figure 8, will give the most ideal response in terms of CIP removal using chitosan-CNT from aqueous solution. Therefore, model validation experimental studies were conducted under the aforementioned optimum conditions at 95% confidence prediction level, 64.38% CIP removal was obtained at a standard deviation of 0.369%. The low standard deviation suggests that the application of the CCD in RSM demonstrated a good correspondence between experimental and predicted values.

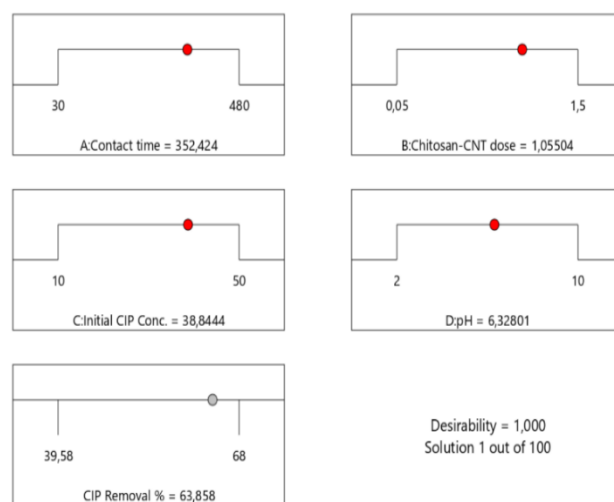


**Figure 8.** Ramp plot for numerical optimization conditions

Table 4 depicts findings of the present study and work reported in literature on CIP removal from aqueous solution using chitosan-based adsorbents. Wang et al. [6] investigated the sorption of CIP on novel magnetised chitosan grafted graphene oxide (MCGO) composite at varying solution pH. The chitosan composite was magnetised using iron oxide ( $\text{Fe}_3\text{O}_4$ ) for easy separation. Wang and co-workers reported a significant decrease in the sorption of CIP on MCGO at  $\text{pH}>5$ . The observed trend was ascribed to the decrease in the weakening of positive charges on the surface of the model adsorbent subsequently resulting in significant repulsion forces between the anionic CIP and MCGO composite. On the other hand, Verma et al. [14] investigated the sorption of CIP on graphene oxide functionalised chitosan (CSGO) composite. The chitosan grafting with graphene oxide was done through the nucleophilic addition and elimination reaction between the graphene oxide  $-\text{COOH}$  group and the  $-\text{NH}_2$  group of chitosan [14]. Highest CIP removal  $>80\%$  was reported for a solution pH range of 4-6 [14]. The observed adsorption behaviour was ascribed to the solution pH and speciation nature of CIP. It is worth noting that Verma et al. [14] reported that for solution pH values greater than 8.7, CIP is negatively charged, thus compromising its interaction with the negatively charged CSGO surface due to an increase in repulsion forces resulting in low adsorption efficiencies of CIP. As such, a similar CIP adsorption trend was observed by Rasoulzadeh et al. [13] and Nazraz et al. [15] using magnetite imprinted chitosan (Fe-CS) nanocomposite ( $\text{pH}=7$ ) and magnesium oxide, chitosan, and graphene oxide (MgO/CS/GO) nanocomposite ( $\text{pH}=6.5$ ), respectively.

**Table 4.** Experimental conditions and adsorption of CIP on chitosan composite from aqueous solutions

Adsorbent	pH	Removal Efficiency (%)	Reference
MCGO	5	$>80$	[6]
CGO	4	$>90$	[14]
MgO/CS/GO	7	$>80$	[15]
$\text{Fe}_3\text{O}_4$ -chitosan	9	99	[16]
Fe-CS	6.5	68	[13]
Chitosan-CNT	6.3	64	Present study

On the other hand, Yadav et al. [16] reported an optimum pH of 9 for  $>99\%$  CIP removal using magnetite ( $\text{Fe}_3\text{O}_4$ ) functionalised chitosan composite ( $\text{Fe}_3\text{O}_4$ -chitosan). Optimum solution pH values of 7 and 8 were reported for tetracycline (TC) and doxycycline (DC), respectively. As such, the findings reported by Yadav et al. [16] suggests that pH variation alters both the model adsorbent surface charge and the charge distribution of targeted pollutant compounds in aqueous solution. The observed sorption trend under weak acidic and basic aqueous environment is attributed to the compromised stability of antibiotics in the context of CIP under strong acidic and/or basic conditions [16]. Moreover, the conditions reported by Yadav et al. [16] suggest that the deprotonation of the model chitosan composite surface functional groups was slow with an increase in solution pH compared to CIP functional moieties. Generally, in alkaline pH aqueous environments antibiotics including CIP acquire a negative charge hence, at weak acidic and neutral pH conditions cationic and zwitterionic are the dominating ionic forms of antibiotics with  $\pi$  electron acceptors. The presence of the  $\pi$  electron acceptors promote the adsorption of antibiotics by the  $\pi - \pi$  electron donor-acceptor interaction mechanism [16], while the rise in pH hinders the adsorption of antibiotics

by the pie extraction mechanism. Therefore, the slow deprotonation of the adsorbent surface with an increase in pH can favour the sorption of antibiotics by electrostatic interaction under weak alkaline conditions as demonstrated by Yadav et al. [16] with a significant CIP removal of 99%.

On the other hand, the current study recorded 64% CIP removal under optimum pH conditions of 6.3, which is within the reported optimum pH range of 4-9 reported in studies [6, 13-16]. It is worth noting that the current study and the work reported by Rasoulzadeh et al. [13] recorded  $>70\%$  CIP removal at an optimum pH of 6.3 and 6.5, respectively. The low CIP removal when compared to the work reported by Wang et al. [6], Verma et al. [14], Nazraz et al. [15], and Yadav et al. [16] can be ascribed to the low oxygen functional groups i.e.,  $-\text{OH}$  on the surface of the Fe-CS and chitosan-CNT adsorbent which protonates and deprotonates under varying pH conditions. Whereas the high CIP removal of  $>80\%$  for the studies presented in Table 4 can be ascribed to the high concentration of  $-\text{OH}$  groups on the surface of the model chitosan composites. The findings of the current study suggest that there was significant deprotonation of the model adsorbent surface functional moieties with an increase in pH (i.e.,  $\text{pH}>6.3$ ), thus hindering the adsorption of CIP both by pie interaction and/or electrostatic mechanism.

#### 4. CONCLUSION AND FUTURE PERSPECTIVES

From the results obtained, it is apparent that the sorption of CIP on chitosan-CNT adsorbent could be modelled by RSM using the reduced cubic polynomial model. The significance of the model in predicting the adsorption of CIP on chitosan-CNT composite was cemented by the obtained model statistical parameters of  $R^2=0.9967$ , adjusted  $R^2=0.9950$ , and predicted  $R^2=0.9552$ . All investigated model independent variables had a significant effect on CIP adsorption in the order of  $\text{pH}>\text{initial CIP concentration}>\text{adsorbent dose}>\text{contact time}$ , recording p-values less than 0.05. From the findings of the current study, it is apparent that the solution pH has a significant effect on the sorption of CIP on chitosan-CNT compared to CIP initial concentration, adsorbent dose as well as contact time. The observed trend can be ascribed to the effect of pH on the adsorbent surface charge as well as CIP speciation. The model numerical optimization results gave 100 possible solutions and a desirability of 1, as such the optimum conditions for CIP removal generated by RSM were obtained at  $\text{pH}=6.3$ , adsorbent dose= $1.06 \text{ g/L}$ , contact time= $352$  minutes, and initial CIP concentration= $39 \text{ mg/L}$ . The aforementioned optimum conditions recorded CIP removal of 64.3% with a prediction error of 0.396% in terms of standard deviation. The generated CIP removal predictive model within the framework of RSM only considered significant interactive model terms i.e., A, B, C, D, AB, AC, AD, BC, BD, CD,  $A^2$ ,  $B^2$ ,  $D^2$ , and  $AB^2$ . Moreover, the findings of the present work are congruent to previously done studies on CIP sorption on chitosan composites under different CIP initial concentration and solution pH [13, 15]. Therefore, the findings of the present study suggest that the model adsorbent can be employed in the sorption of antibiotics under different solution pH and adsorbate initial concentration conditions from aqueous environments. However, it is worth noting that the solution pH has demonstrated to have a significant effect on the speciation of antibiotics in solution, as such each antibiotic can behave differently depending on the  $\text{pK}_a$  value for each antibiotic.

It is worth noting that for the current study other effects that may have an adsorption effect if CIP on the model adsorbent such as coexistence of competing ions, adsorbent generation, as well as temperature effects were not investigated for the current study. The aforementioned factors can be considered for future perspectives on the basis that the current study is focusing on model optimization.

## ACKNOWLEDGMENT

This work was supported by the Green Engineering Research Group at the Durban University of Technology. The work was also supported by the South African National Research Fund under the research development grant for Y-rated researchers, grant number 137765.

## REFERENCES

- [1] Foureaux, A.F.S., Reis, E.O., Lebron, Y., Moreira, V., Santos, L.V., Amaral, M.S., Lange, L.C. (2019). Rejection of pharmaceutical compounds from surface water by nanofiltration and reverse osmosis. *Separation and Purification Technology*, 212: 171-179. <https://doi.org/10.1016/j.seppur.2018.11.018>
- [2] Chander, V., Sharma, B., Negi, V., Aswal, R., Singh, P., Singh, R., Dobhal, R. (2016). Pharmaceutical compounds in drinking water. *Journal of Xenobiotics*, 6(1): 5774. <https://doi.org/10.4081/xeno.2016.5774>
- [3] Lyu, J., Yang, L.S., Zhang, L., Ye, B.X., Wang, L. (2020). Antibiotics in soil and water in China-A systematic review and source analysis. *Environmental Pollution*, 266: 115147. <https://doi.org/10.1016/j.envpol.2020.115147>
- [4] Mhuka, V., Dube, S., Nindi, M.M. (2020). Occurrence of pharmaceutical and personal care products (PPCPs) in wastewater and receiving waters in South Africa using LC-Orbitrap™ MS. *Emerging Contaminants*, 6: 250-258. <https://doi.org/10.1016/j.emcon.2020.07.002>
- [5] Madikizela, L.M., Tavengwa, N.T., Chimuka, L. (2017). Status of pharmaceuticals in African water bodies: Occurrence, removal and analytical methods. *Journal of Environmental Management*, 193: 211-220. <https://doi.org/10.1016/j.jenvman.2017.02.022>
- [6] Wang, F., Yang, B.S., Wang, H., Song, Q.X., Tan, F.J., Cao, Y.A. (2016). Removal of ciprofloxacin from aqueous solution by a magnetic chitosan grafted graphene oxide composite. *Journal of Molecular Liquids*, 222: 188-194. <https://doi.org/10.1016/j.molliq.2016.07.037>
- [7] Ma, X., Wang, Z.J. (2022). Removal of ciprofloxacin from wastewater by ultrasound/electric field/sodium persulfate (US/E/PS). *Processes*, 10(1): 124. <https://doi.org/10.3390/pr10010124>
- [8] Abd El-Monaem, E.M., Eltaweil, A.S., Elshishini, H.M., Hosny, M., Abou Alsoaud, M.M., Attia, N.F., El-Subruiti, G.M., Omer, A.M. (2022). Sustainable adsorptive removal of antibiotic residues by chitosan composites: An insight into current developments and future recommendations. *Arabian Journal of Chemistry*, 15(5): 103743. <https://doi.org/10.1016/j.arabjc.2022.103743>
- [9] Avcı, A., İnci, İ., Baylan, N. (2020). Adsorption of ciprofloxacin hydrochloride on multiwall carbon nanotube. *Journal of Molecular Structure*, 1206: 127711. <https://doi.org/10.1016/j.molstruc.2020.127711>
- [10] Bair, D.A., Anderson, C.G., Chung, Y., Scow, K.M., Franco, R.B., Parikh, S.J. (2020). Impact of biochar on plant growth and uptake of ciprofloxacin, triclocarban and triclosan from biosolids. *Journal of Environmental Science and Health, Part B*, 55(11): 990-1001. <https://doi.org/10.1080/03601234.2020.1807264>
- [11] Afzal, M.Z., Sun, X.F., Liu, J., Song, C., Wang, S.G., Javed, A. (2018). Enhancement of ciprofloxacin sorption on chitosan/biochar hydrogel beads. *Science of the Total Environment*, 639: 560-569. <https://doi.org/10.1016/j.scitotenv.2018.05.129>
- [12] de Almeida, A.D.S.V., de Figueiredo Neves, T., da Silva, M.G.C., Prediger, P., Vieira, M.G.A. (2022). Synthesis of a novel magnetic composite based on graphene oxide, chitosan and organoclay and its application in the removal of bisphenol A, 17 $\alpha$ -ethinylestradiol and triclosan. *Journal of Environmental Chemical Engineering*, 10(1): 107071. <https://doi.org/10.1016/j.jece.2021.107071>
- [13] Rasoulzadeh, H., Mohseni-Bandpei, A., Hosseini, M., Safari, M. (2019). Mechanistic investigation of ciprofloxacin recovery by magnetite-imprinted chitosan nanocomposite: Isotherm, kinetic, thermodynamic and reusability studies. *International Journal of Biological Macromolecules*, 133: 712-721. <https://doi.org/10.1016/j.ijbiomac.2019.04.139>
- [14] Verma, M., Lee, I., Sharma, S., Kumar, R., Kumar, V., Kim, H. (2021). Simultaneous removal of heavy metals and ciprofloxacin micropollutants from wastewater using ethylenediaminetetraacetic acid-functionalized  $\beta$ -cyclodextrin-chitosan adsorbent. *ACS Omega*, 6(50): 34624-34634. <https://doi.org/10.1021/acsomega.1c05015>
- [15] Nazraz, M., Yamini, Y., Asiabi, H. (2019). Chitosan-based sorbent for efficient removal and extraction of ciprofloxacin and norfloxacin from aqueous solutions. *Microchimica Acta*, 186: 1-9. <https://doi.org/10.1007/s00604-019-3563-x>
- [16] Yadav, P., Yadav, A., Labhasetwar, P.K. (2022). Sustainable adsorptive removal of antibiotics from aqueous streams using Fe<sub>3</sub>O<sub>4</sub>-functionalized MIL101 (Fe) chitosan composite beads. *Environmental Science and Pollution Research*, 29(25): 37204-37217. <https://doi.org/10.1007/s11356-021-18385-3>
- [17] Sekimoto, T., Nishihama, S., Yoshizuka, K., Maeda, R. (2018). Adsorptive removal of sulfamethoxazole with shell-core chitosan immobilized metal ion. *Separation Science and Technology*, 53(7): 1116-1123. <https://doi.org/10.1080/01496395.2017.1340954>
- [18] Chandrasekaran, A., Patra, C., Narayanasamy, S., Subbiah, S. (2020). Adsorptive removal of ciprofloxacin and amoxicillin from single and binary aqueous systems using acid-activated carbon from *Prosopis juliflora*. *Environmental Research*, 188: 109825. <https://doi.org/10.1016/j.envres.2020.109825>
- [19] Liang, X.X., Omer, A.M., Hu, Z.H., Wang, Y.G., Yu, D., Ouyang, X.K. (2019). Efficient adsorption of diclofenac sodium from aqueous solutions using magnetic amine-functionalized chitosan. *Chemosphere*, 217: 270-278. <https://doi.org/10.1016/j.chemosphere.2018.11.023>
- [20] Niaei, H.A., Rostamizadeh, M. (2020). Adsorption of metformin from an aqueous solution by Fe-ZSM-5 nano-

- adsorbent: Isotherm, kinetic and thermodynamic studies. *The Journal of Chemical Thermodynamics*, 142: 106003. <https://doi.org/10.1016/j.jct.2019.106003>
- [21] Khumalo, S.M., Makhathini, T.P., Bwapwa, J.K., Bakare, B.F., Rathilal, S. (2023). The occurrence and fate of antibiotics and nonsteroidal anti-inflammatory drugs in water treatment processes: A review. *Journal of Hazardous Materials Advances*, 10: 100330. <https://doi.org/10.1016/j.hazadv.2023.100330>
- [22] Zhang, K., Sumita, Li, C., Sun, C.M., Marmier, N. (2022). A review of the treatment process of perfluorooctane compounds in the waters: Adsorption, flocculation, and advanced oxidative process. *Water*, 14(17): 2692. <https://doi.org/10.3390/w14172692>
- [23] Zhao, R., Ma, T.T., Zhao, S., Rong, H.Z., Tian, Y.Y., Zhu, G.S. (2020). Uniform and stable immobilization of metal-organic frameworks into chitosan matrix for enhanced tetracycline removal from water. *Chemical Engineering Journal*, 382: 122893. <https://doi.org/10.1016/j.cej.2019.122893>
- [24] Shah, A.M., Qazi, I.H., Matra, M., Wanapat, M. (2022). Role of chitin and chitosan in ruminant diets and their impact on digestibility, microbiota and performance of ruminants. *Fermentation*, 8(10): 549. <https://doi.org/10.3390/fermentation8100549>
- [25] Thou, C.Z., Khan, F.S.A., Mubarak, N.M., Ahmad, A., Khalid, M., Jagadish, P., Walvekar, R., Abdullah, E.C., Khan, S., Khan, M., Hussain, S., Ahmad, I., Algarni, T.S. (2021). Surface charge on chitosan/cellulose nanowhiskers composite via functionalized and untreated carbon nanotube. *Arabian Journal of Chemistry*, 14(3): 103022. <https://doi.org/10.1016/j.arabjc.2021.103022>
- [26] Carson, L., Kelly-Brown, C., Stewart, M., Oki, A., Regisford, G., Luo, Z., Bakhmutov, V.I. (2009). Synthesis and characterization of chitosan-carbon nanotube composites. *Materials Letters*, 63(6-7): 617-620. <https://doi.org/10.1016/j.matlet.2008.11.060>
- [27] Mallakpour, S., Azadi, E., Hussain, C.M. (2021). Chitosan/carbon nanotube hybrids: recent progress and achievements for industrial applications. *New Journal of Chemistry*, 45(8): 3756-3777. <https://doi.org/10.1039/D0NJ06035F>
- [28] Wang, S.F., Shen, L., Zhang, W.D., Tong, Y.J. (2005). Preparation and mechanical properties of chitosan/carbon nanotubes composites. *Biomacromolecules*, 6(6): 3067-3072. <https://doi.org/10.1021/bm050378v>
- [29] Ji, L.L., Chen, W., Zheng, S.R., Xu, Z.Y., Zhu, D.Q. (2009). Adsorption of sulfonamide antibiotics to multiwalled carbon nanotubes. *Langmuir*, 25(19): 11608-11613. <https://doi.org/10.1021/la9015838>
- [30] Sobczak-Kupiec, A., Drabczyk, A., Florkiewicz, W., Głab, M., Kudłacik-Kramarczyk, S., Słota, D., Tomala, A., Tylińczak, B. (2021). Review of the applications of biomedical compositions containing hydroxyapatite and collagen modified by bioactive components. *Materials*, 14(9): 2096. <https://doi.org/10.3390/ma14092096>
- [31] Montgomery, D.C. (2017). *Design and Analysis of Experiments*. John Wiley & Sons.
- [32] Khumalo, S.M., Bakare, B.F., Tetteh, E.K., Rathilal, S. (2023). Application of response surface methodology on brewery wastewater treatment using chitosan as a coagulant. *Water*, 15(6): 1176. <https://doi.org/10.3390/w15061176>
- [33] Madondo, N.I., Rathilal, S., Bakare, B.F. (2022). Utilization of response surface methodology in optimization and modelling of a microbial electrolysis cell for wastewater treatment using box-behnken design method. *Catalysts*, 12(9): 1052. <https://doi.org/10.3390/catal12091052>
- [34] Bezerra, M.A., Santelli, R.E., Oliveira, E.P., Villar, L.S., Escaleira, L.A. (2008). Response surface methodology (RSM) as a tool for optimization in analytical chemistry. *Talanta*, 76(5): 965-977. <https://doi.org/10.1016/j.talanta.2008.05.019>
- [35] Alimohammadi, M., Saeedi, Z., Akbarpour, B., Rasoulzadeh, H., Yetilmezsoy, K., Al-Ghouti, M.A., Khraisheh, M., McKay, G. (2017). Adsorptive removal of arsenic and mercury from aqueous solutions by eucalyptus leaves. *Water, Air, & Soil Pollution*, 228: 1-27. <https://doi.org/10.1007/s11270-017-3607-y>
- [36] Giraldo, J.D., Rivas, B.L. (2021). Direct ionization and solubility of chitosan in aqueous solutions with acetic acid. *Polymer Bulletin*, 78: 1465-1488. <https://doi.org/10.1007/s00289-020-03172-w>
- [37] Candioti, L.V., De Zan, M.M., Cámara, M.S., Goicoechea, H.C. (2014). Experimental design and multiple response optimization. Using the desirability function in analytical methods development. *Talanta*, 124: 123-138. <https://doi.org/10.1016/j.talanta.2014.01.034>